EAGE

Process-based modelling of turbidity currents: from computational fluid-dynamics to depositional signature

Age J. Vellinga*[1], Matthieu J.B. Cartigny[2], Ernst W.M. Hansen[3], Peter J. Talling[2], Michael A. Clare[2], Esther J. Sumner[1]

[1] University of Southampton, United Kingdom
[2] National Oceanography Centre Southampton, United Kingdom
[3] Complex Flow Design AS, Trondheim, Norway
* a.j.vellinga@soton.ac.uk

Introduction

Turbidity currents are amongst the most important sediment transport processes, and form the largest sedimentary bodies on our planet (Talling et al., 2012). These deposits hold a significant share of hydrocarbon reservoirs worldwide (Stow and Johansson, 2000). Surprisingly little is known about turbidity currents and their deposits; turbidites, despite their impressive scale and economic importance.

Current knowledge on how turbidites form is heavily reliant on inferences made from outcrop studies, numerical models and scaled physical experiments, as turbidity currents are notoriously difficult to observe directly (Talling et al., 2015). Outcrop studies provide valuable large-scale detailed information on turbidites, however, the link to formative processes remains speculative, as different flow types may produce similar deposits. Scaled laboratory experiments provide an important aide to understand the inner mechanics of turbidity currents, but scaling limitations mean processes observed in laboratory do not fully represent the processes operating at full scale (Talling et al., 2012). Numerical modelling can be a useful tool in understanding how fluid-processes interact with the bed, but have mainly used depth-averaged models, which cannot provide insight into the vertical velocity and concentration structure of the flow, yet these parameters are key to link flow processes to their deposits.

From a hydrocarbon perspective, understanding turbidite reservoir architecture and facies heterogeneity is important, as multi-million dollar decisions regarding field-development are based on these interpretations. Seismic data have decametre-scale resolution, and even in combination with well data provide limited insight into smaller-scale and facies heterogeneity. Geostatistical methods used in static reservoir modelling use spatial continuity functions that are conditioned by analogues, hence such methods only indirectly include sedimentary processes, and have therefore limited capabilities to predict deposit characteristics in between wells (Pyrcz et al., 2014).

In this study, a process-based depth-resolved forward model is employed, to investigate the dynamics of turbidity currents, their interaction with the seafloor, and their resulting deposits. The depth-resolved property of the applied computational fluid-dynamic (CFD) code, provides a detailed image of flow-velocity, sediment-concentration, and other flow properties, varying trough space and time. This method allows for a quantification of erosional and depositional patterns, thereby capturing both depositional architectures and the internal facies heterogeneity. The aim here is to model the depositional signature of turbidity currents with specific characteristics, on a metre-scale, thereby allowing for the first time a quantification of the link between flow dynamics, depositional architecture and internal facies distribution.

Methodology

Depositional architecture and facies are linked to flow dynamics as depositional and erosional processes are fully resolved. The fluid-flow and sediment-transport processes necessary to model erosion and deposition in the model are briefly explained here. To simulate fluid-motion, FLOW-3D®, a Reynolds-Averaging Navier-Stokes (RANS) model, is used. The model computes the three-dimensional fluid motion by solving the mass and momentum balances over the computational cells.

As sub-cell-scale motions are not directly simulated, a turbulence model is used to account for turbulence effects at sub-grid-scale. The applied turbulence model is a two-equation k-ε model, based upon the turbulent viscosity hypothesis, which assumes that momentum transferred by turbulent

eddies can be modelled using an eddy viscosity, and solves two equations, for (1) turbulent kinetic energy and (2) turbulent dissipation, further details on the model can be found in Basani et al. (2014).

The sediment transport model

Sediment grains are not modelled individually, instead, fluxes of sediment between computational cells are estimated using sediment transport models. Bed-load transport and suspended-load transport are modelled individually.

Bed-load transport is modelled using the empirical approach of Meyer-Peter and Müller (1948) to calculate a bed-load flux (Eq. 1), where f_s is the fraction of a given sediment species, β a bed-load coefficient, θ and θ_{cr} are the local and critical Shields parameters, ρ_s and ρ_f the densities of sediment and water, g the acceleration due to gravity and d_s the grain-size.

$$q_b = f_s \beta (\theta_i - \theta_{cr})^{1.5} \sqrt{g\left(\frac{\rho_s - \rho_f}{\rho_f}\right) d_s^3} \qquad \text{(Eq. 1)}$$

Suspended load transport is modelled by accounting for (1) entrainment of sediment into suspension, (2) drift and settling of the sediment, and (3) advection and dispersion of the sediment. Sediment entrainment is quantified by a lift velocity (Eq. 2; Winterwerp et al., 1992), where α is an entrainment coefficient, $\boldsymbol{n}$ a bed-normal vector, and d_* a dimensionless grain-size parameter.

$$\boldsymbol{u_{lift}} = \alpha \boldsymbol{n} d_*^{0.3} (\theta_i - \theta_{cr})^{1.5} \sqrt{\frac{\|g\| d (\rho_s - \rho_f)}{\rho_f}} \qquad \text{(Eq. 2)}$$

The combination of settling due to gravity, and the flow-parallel movement due to the drag exerted on the sediment by the fluid flow, is expressed in the drift velocity ($\boldsymbol{u_{drift}}$). The relative velocity between water and sediment is computed using momentum-balance and mass-balance equations of the mixture (Eq. 3, 4 and 5), where subscripts *f* and *s* refer to fluid and sediment, *f* is the fraction of either fluid or sediment, *F* refers to the gravity force, and *K* is a drag-function combining drag and Stokes's drag.

$$\bar{\boldsymbol{u}} = f_f \boldsymbol{u_f} + f_s \boldsymbol{u_s} \quad \text{such that} \quad \nabla \cdot \bar{\boldsymbol{u}} = 0 \qquad \text{(Eq. 3)}$$

$$\frac{\partial \boldsymbol{u_f}}{\partial t} + \boldsymbol{u_f} \cdot \nabla \boldsymbol{u_f} = -\frac{1}{\rho_f} \nabla p + F + \frac{K}{f_f \rho_f} \boldsymbol{u_r} \qquad \text{(Eq. 4)}$$

$$\frac{\partial \boldsymbol{u_s}}{\partial t} + \boldsymbol{u_s} \cdot \nabla \boldsymbol{u_s} = -\frac{1}{\rho_s} \nabla p + F + \frac{K}{f_s \rho_s} \boldsymbol{u_r} \qquad \text{(Eq. 5)}$$

The drift velocity (Eq. 6) is the difference in velocity between the mean velocity of the fluid-sediment mixture ($\boldsymbol{u}$) and relative velocity ($\boldsymbol{u_r}$).

$$\boldsymbol{u_{drift}} = \bar{\boldsymbol{u}} - \boldsymbol{u_r} \qquad \text{(Eq. 6)}$$

Sediment in suspension is advected, as it moves with the bulk motion of the flow, and dispersed due to turbulence in a diffusion-like process. These processes are described by equation 7, in which the left-had side denotes advection and the right hand side diffusion, where *D* is a diffusion coefficient related to the turbulence model.

$$\frac{\partial C}{\partial t} + \nabla \cdot (\boldsymbol{u} C) = \nabla \cdot \nabla (D C) \qquad \text{(Eq. 7)}$$

An example study

Here we describe an individual flow in more detail to demonstrate how this numerical model can now be used to directly study the link between flow processes and the resulting deposit in a large scale simulation. The simulated domain is 1 km in length, and has a step-like morphology (Fig. 1A), loosely based on the morphology of the Shepard's Meander in the Monterey Canyon, offshore California, as described by Fildani et al. (2006). The bed has a median grain size of 125µm. The simulated domain consists of 1500 by 150 cells with Resolution of 67cm in the x-direction and 20cm in the z-direction. A dilute turbidity current, with an average sediment concentration of 1.13%

(30kg/m^3), half of it silt-sized material and the other half split evenly between grain-sizes of 50µm, 100µm and 150µm, an initial flow thickness of 5 metre, and mean velocity of 2 m/s, is simulated, and flows over the pre-defined morphology. Apart from the initial and boundary conditions, there are no constrains on the development of either the turbidity current or the bed, hence the flow can either deposit or erode, depending on local flow conditions.

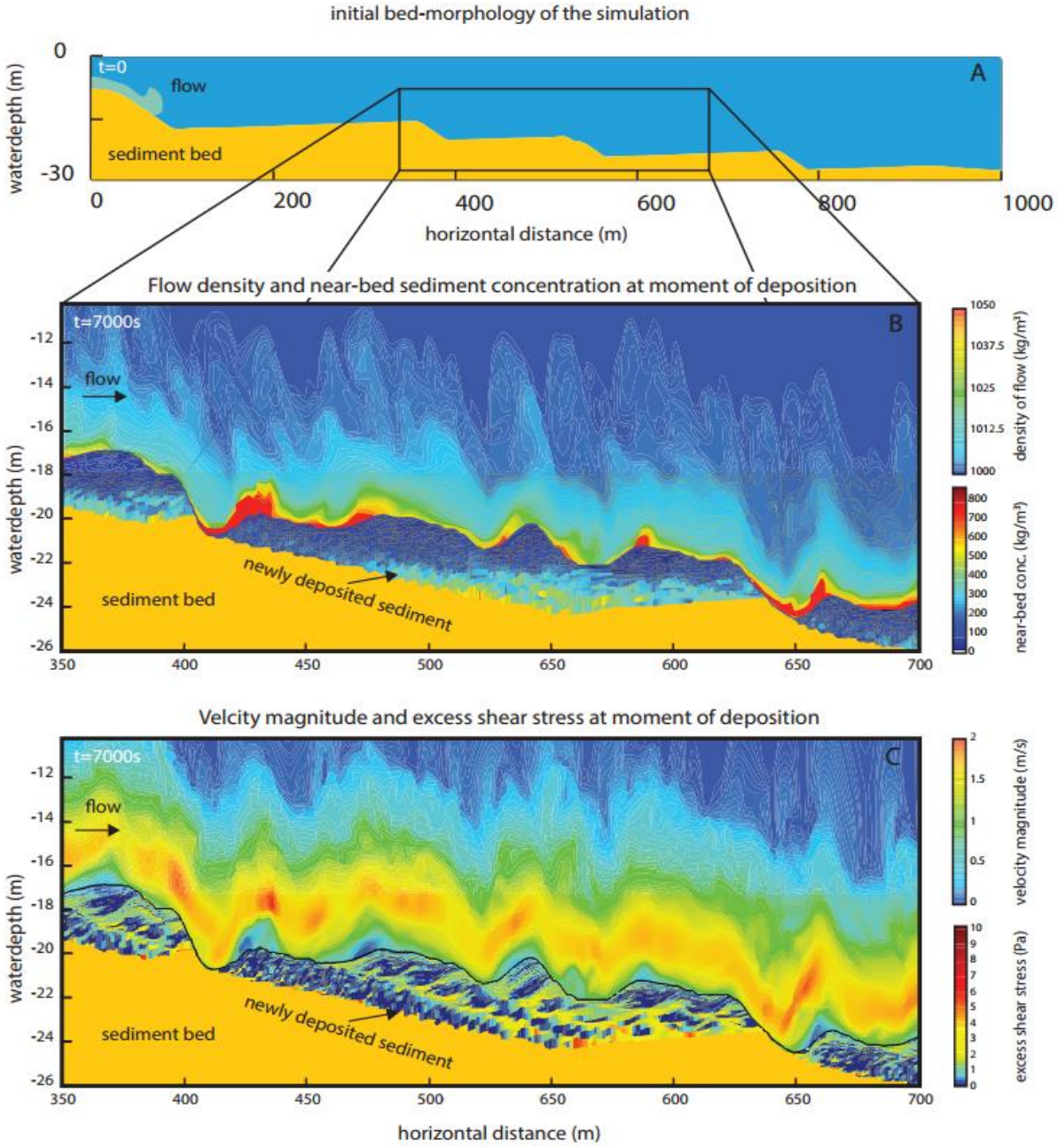

Figure 1 *The initial condition of the bed; a mean slope of 0.015 with a step-like morphology (panel A). The other panels are zoom-ins of the bed at t=7000s, showing flow density (B) and velocity magnitude (C) snapshots at t=7000s, and near-bed sediment concentration (B) and shear stress (C) at the moment a sediment parcel got deposited.*

After a 2-hour sustained turbidity current, the turbidity current has eroded the bed in some places, the steeper areas where shear velocities were higher, and deposited sediment on the horizontally-emplaced steps. In more detail, a series of sediment waves appears to have formed on the horizontally oriented steps (Fig. 1B, C).

Panels B and C in Fig. 1 are just an example of some of the properties of both the flow and the bed that can be displayed; flow density, dependent on sediment concentration, and flow velocity

magnitude. The turbidity current accelerates over the steeper areas, at x=400m for example. The flow decreases in average velocity at the more horizontal parts, and displays a distinct velocity field with complex flow structures near the bed. An increase in flow thickness, especially of the denser part, can be observed as well. Concentration and velocity profiles vary significantly over the flow through space and time, and such detail is required to simulate bed-development.

Depositional patterns emerge in Fig. 1. In the case of shear stresses: there is no image on the shear stresses at moment of deposition at the steeper steps, as these are erosive. At the smaller-scale sediment waves, emplaced on the more horizontal steps, low shear stresses are observed on the upstream-flanks, and higher shear-stresses on the downstream flanks, explaining preferential deposition on the upstream flank. The sediment concentration at the moment of deposition is relatively high for the initial deposits, and deposits are relatively thick, likely caused by an erosive head of the current increasing sediment concentrations. Internal patterns in the deposited sediment emerge as different properties are displayed, which can help interpret sedimentary processes as flow data is available, or can be translated into facies patterns and maps.

Conclusions

Here we show that it is feasible to study the link between flow dynamics and flow deposits by the use of a numerical model. This method is able to produce detailed facies maps, to find generalised depositional signatures of flows with different characteristics. Additionally, the method aides a better understanding of processes shaping bed-morphologies and deposits, as flow-conditions at the flow-bed interface are known over time and space. We envision that such process-based modelling approaches can in future be used to improve geostatistical reservoir-modelling tools.

Acknowledgements

A special thanks to ExxonMobil for financing this study, and Complex Flow Design AS to allow the use of their computational capabilities.

References

Basani, R., Janocko, M., Cartigny, M.J.B., Hansen, W.M., and Eggenhuisen, J.T., 2014, MassFLOW-3D TM as a simulation tool for turbidity currents : some preliminary results: IAS Speical Publication, v. 46, p. 587–608.

Fildani, A., Normark, W.R., Kostic, S., and Parker, G., 2006, Channel formation by flow stripping: large-scale scour features along the Monterey East Channel and their relation to sediment waves: Sedimentology, v. 53, no. 6, p. 1265–1287, doi: 10.1111/j.1365-3091.2006.00812.x.

Meyer-Peter, E. and Müller, R., 1948, Formulas for Bed-Load Transport, *in* International Association for Hydraulic Structures Research - Second Meeting, p. 7–9. VI.

Pyrcz, M., Sech, R., Covault, J., Sun, T., Willis, B., and Sylvester, Z., 2014, Process-mimicking Modeling Considerations, *in* Closing the gap II: advances in applied geomodelling for hydrocarbon reservoirs, p. 1–16.

Stow, D. a. ., and Johansson, M., 2000, Deep-water massive sands: nature, origin and hydrocarbon implications: Marine and Petroleum Geology, v. 17, no. 2, p. 145–174, doi: 10.1016/S0264-8172(99)00051-3.

Talling, P.J., Allin, J., Armitage, D. a, Arnott, R.W.C., Cartigny, M.J.B., Clare, M. a, Felletti, F., Covault, J. a, Girardclos, S., Hansen, E., Hill, P.R., Hiscott, R.N., Hogg, A.J., Clarke, J.H., et al., 2015, Key Future Directions for Research on Turbidity Currents and Their Deposits: Journal of Sedimentary Research, v. 85, no. February, p. 153–169, doi: 10.2110/jsr.2015.03.

Talling, P.J., Masson, D.G., Sumner, E.J., and Malgesini, G., 2012, Subaqueous sediment density flows: Depositional processes and deposit types: Sedimentology, v. 59, no. 7, p. 1937–2003, doi: 10.1111/j.1365-3091.2012.01353.x.

Winterwerp, J.C., de Groot, M.B., Masebrgens, D.R., and Verwoert, H., 1992, Hyperconcentrated sand-water mixutre flows over erodible bed: Journal of Hydraulic Engineering, v. 118, no. 11, p. 1508–1525.